RESEARCH ARTICLE | JUNE 05 2023

Constructive role of shot noise in the collective dynamics of neural networks ⊘

Special Collection: Regime switching in coupled nonlinear systems: sources, prediction, and control

V. V. Klinshov ✉ ; P. S. Smelov ; S. Yu. Kirillov

🔘 Check for updates

🌐 View Online

↗ Export Citation

CrossMark

Articles You May Be Interested In

Shot-to-shot reproducibility of a self-magnetically insulated ion diode

Rev Sci Instrum (July 2012)

Shot to shot variation in perveance of the explosive emission electron beam diode

Physics of Plasmas (March 2009)

Shot-by-shot spectrum model for rod-pinch, pulsed radiography machines

AIP Advances (February 2018)

Constructive role of shot noise in the collective dynamics of neural networks

View Online   Export Citation   CrossMark

V. V. Klinshov,[1,2,a] P. S. Smelov,[1] and S. Yu. Kirillov[1,b]

AFFILIATIONS

[1] Institute of Applied Physics of the Russian Academy of Sciences, Ulyanova Street 46, 603950 Nizhny Novgorod, Russia
[2] National Research University Higher School of Economics, 25/12 Bol'shaya Pecherskaya Street, Nizhny Novgorod 603155, Russia

Note: This paper is part of the Focus Issue on Regime switching in coupled nonlinear systems: sources, prediction, and control.
[a] **Author to whom correspondence should be addressed:** vladimir.klinshov@ipfran.ru
[b] **Electronic mail:** skirillov@ipfran.ru

ABSTRACT

Finite-size effects may significantly influence the collective dynamics of large populations of neurons. Recently, we have shown that in globally coupled networks these effects can be interpreted as additional common noise term, the so-called shot noise, to the macroscopic dynamics unfolding in the thermodynamic limit. Here, we continue to explore the role of the shot noise in the collective dynamics of globally coupled neural networks. Namely, we study the noise-induced switching between different macroscopic regimes. We show that shot noise can turn attractors of the infinitely large network into metastable states whose lifetimes smoothly depend on the system parameters. A surprising effect is that the shot noise modifies the region where a certain macroscopic regime exists compared to the thermodynamic limit. This may be interpreted as a constructive role of the shot noise since a certain macroscopic state appears in a parameter region where it does not exist in an infinite network.

The collective dynamics of large populations of active units in certain cases can be reduced to low-dimensional dynamical systems for averaged variables. In the case of neural networks, such reduced systems are called neural mass models. These models are exact in the limit of infinitely large networks, while finite size effects lead to deviations between the neural mass model and the full system describing the microscopic dynamics. For globally coupled networks, such deviations can be interpreted as the action of a common noise signal. Since the origin of this random-like signal is the discrete rather than continuous nature of the population, we call it the "shot noise." In the present paper, we show that this noise can modify the regions of existence of dynamical regimes of the network. As a consequence, certain macroscopic states might appear in a parameter region where it does not exist in the thermodynamic limit, which is interpreted as a constructive role of the shot noise.

I. INTRODUCTION

The electrical activity of neuronal populations provides a substrate for information processing and cognitive functions in the central neural system. Many efforts have been made to better understand the collective behavior of large-scale neural networks, and mathematical modeling has been a guide on this way for several decades. Using models of coupled spiking neurons, a number of important effects have been studied, including synchronization of neural populations,[1–6] asynchronous states,[7,8] periodic collective oscillations,[9–11] microscopic chaos,[12–14] collective irregular dynamics,[15,16] working memory,[17,18] and many others.

A common way to describe the macroscopic dynamics of large-scale neural networks is to deal with macroscopic observables instead of microscopic variables. In some cases, it is possible to write a closed set of equations for the macroscopic variables and to obtain the so-called neural mass model. Such models can be postulated heuristically[19–21] or derived from the microscopic equations.[22–30] Some of the methods to derive neural mass models involve using Ott–Antonsen *Ansatz*[31,32] or Lorentzian *Ansatz*.[33] These techniques are applicable to networks of θ-neurons[34,35] or quadratic integrate-and-fire (QIF) neurons[33] and allow to obtain a low-dimensional set of ODEs for macroscopic variables (or order parameters) of the network. These systems are much simpler for both analytical and

numerical studies than the microscopic models, which makes them very popular in many contexts.[36–44]

It is known that Ott–Antonsen *Ansatz* and Lorentzian *Ansatz* provide exact solutions for the microscopic dynamics in the thermodynamic limit, i.e., when the number of elements is infinite. For large but finite systems, these solutions become approximate, and deviations between the neural mass model and the microscopic model emerge. In our recent paper,[45] we demonstrated that these deviations can be modeled as stochastic fluctuations, which we called "shot noise" in analogy to electronic systems. Adding this noise (which is global in the case of globally coupled networks) to a neural mass model transforms the latter into a set of stochastic differential equations capable of describing finite-size effects in the network. Note that the shot noise appears *only* in the macroscopic dynamics as an approximation, while the system describing the microscopic dynamics is deterministic.

Adding noise to dynamical systems might result in many nontrivial phenomena such as coherence and stochastic resonance, noise-induced oscillations, stochastic synchronization, and noise-induced phase transitions (see Ref. 46 for a review). Since shot noise is inevitable in neural networks, it is important to understand its role in their collective dynamics and to compare it with that of a genuine noise derived from the microscopic level. Previously,[45] we have demonstrated the emergence of pronounced noise-induced collective oscillations due to resonance effects. In the present work, we continue to investigate the shot noise and analyze its ability to induce switching between macroscopic dynamical regimes of the network.

Noise-induced switching in multistable dynamical systems is a widely known phenomenon first studied in the classical paper of Kramers[47] and later observed in many other examples.[48–54] Adding noise to a multistable system turns its attractors into metastable states whereby the system spends some time in vicinity of a state before switching to another one. The lifetime of the metastable state is the key measure of the switching behavior.

In the present paper, we study the switching dynamics due to shot noise and associated lifetimes of metastable states in a finite-size purely excitatory network of globally coupled quadratic integrate-and-fire neurons with most of the neurons in the sub-threshold regime. In the limit of infinitely many neurons, the network can be exactly reduced to the deterministic neural mass model[33] where the only possible stable solutions are fixed points and show no switching. In a certain parameter area, the network is bistable with infinite lifetimes of both the macroscopic regimes. For finite network size, these regimes might become metastable, and we study their lifetimes depending on the network size and its macroscopic parameters. We demonstrate that the lifetime shows a smooth transition from extremely large values when the regime is effectively stable to very small values when the regime effectively vanishes. For large networks, these transitions are abrupt and located near the bifurcation points of the thermodynamic system. For smaller networks, the transitions become smoother and move away from the bifurcation points. The most unexpected finding is that the transition boundaries can shift in such a way that the regime's region of stability expands with respect to that of the thermodynamic case. In other words, shot noise not only smooths the bifurcation transition, but also shifts it and creates a macroscopic state in the parameter region where it does not exist in the deterministic case. This phenomenon shows that the shot noise can play a constructive role in the collective dynamics of neural networks.

II. EXACT SYSTEM AND THE NEURAL MASS MODEL

We consider a *purely excitatory* network of N quadratic integrate-and-fire (QIF) neurons[55,56] with most of the neurons being *sub-threshold*,

$$\dot{V}_j = V_j^2 + \eta_j + Js(t) + I(t). \tag{1}$$

Here, V_j is the membrane potential of the j-neuron, η_j is a heterogeneous bias current, $I(t)$ is a common time-dependent external input that we set to zero in the rest of the paper, J is the coupling strength, and $s(t)$ is the recurrent input,

$$s(t) = \frac{1}{N} \sum_{j=1}^{N} \sum_{k} \delta(t - t_j^k). \tag{2}$$

In (2), t_j^k is the moment of the kth spike of the jth neuron, and $\delta(t)$ describes the postsynaptic current after a single spike (note that we assume infinitely short pulses which is important for further analysis since pulses of finite duration can induce collective oscillations in the network[57,58]). Each neuron emits a spike when its potential V_j reaches the threshold value V_p, after which it is reset to V_r. It is common to set $V_p = -V_r = \infty$ since V_j can reach infinity in finite time due to quadratic nonlinearity in Eq. (1).

Montbrió, Pazó, and Roxin showed that in the thermodynamic limit $N \rightarrow \infty$ the collective behavior of the network can be reduced to a neural mass model for macroscopic variables.[33] The reduction turns out to be especially effective when the bias currents η_j are assumed to have Lorentzian distribution

$$g(\eta) = \frac{1}{\pi} \frac{\Delta}{\Delta^2 + (\eta - \zeta)^2}, \tag{3}$$

where ζ is the mean and Δ is the half-width. In this case, the network dynamics is reduced to just two ODEs,

$$\dot{r} = \Delta/\pi + 2rv, \tag{4a}$$

$$\dot{v} = v^2 + \zeta - \pi^2 r^2 + Jr, \tag{4b}$$

where r is the mean firing rate of the neurons and v is the mean membrane potential. System (4) is exact for infinitely large networks and also provides a reasonable approximation for large but finite networks in many cases. The only possible stable solutions of this system are fixed points, as shown in Ref. 33. It is important to investigate the applicability conditions of this approximation and find out when the finite-size effects lead to substantial deviations between the dynamics of the neural network (1) and its neural mass representation (4).

In our recent work, we have demonstrated that finite size effects can be captured by adding a stochastic term to the neural mass dynamics.[45] The power spectrum of the shot noise might contain pronounced peaks; therefore, it might cause notable oscillations due to resonance effects. Another typical stochastic effect is noise-induced switching between different attractors of the deterministic system. Below we focus on the latter effect.
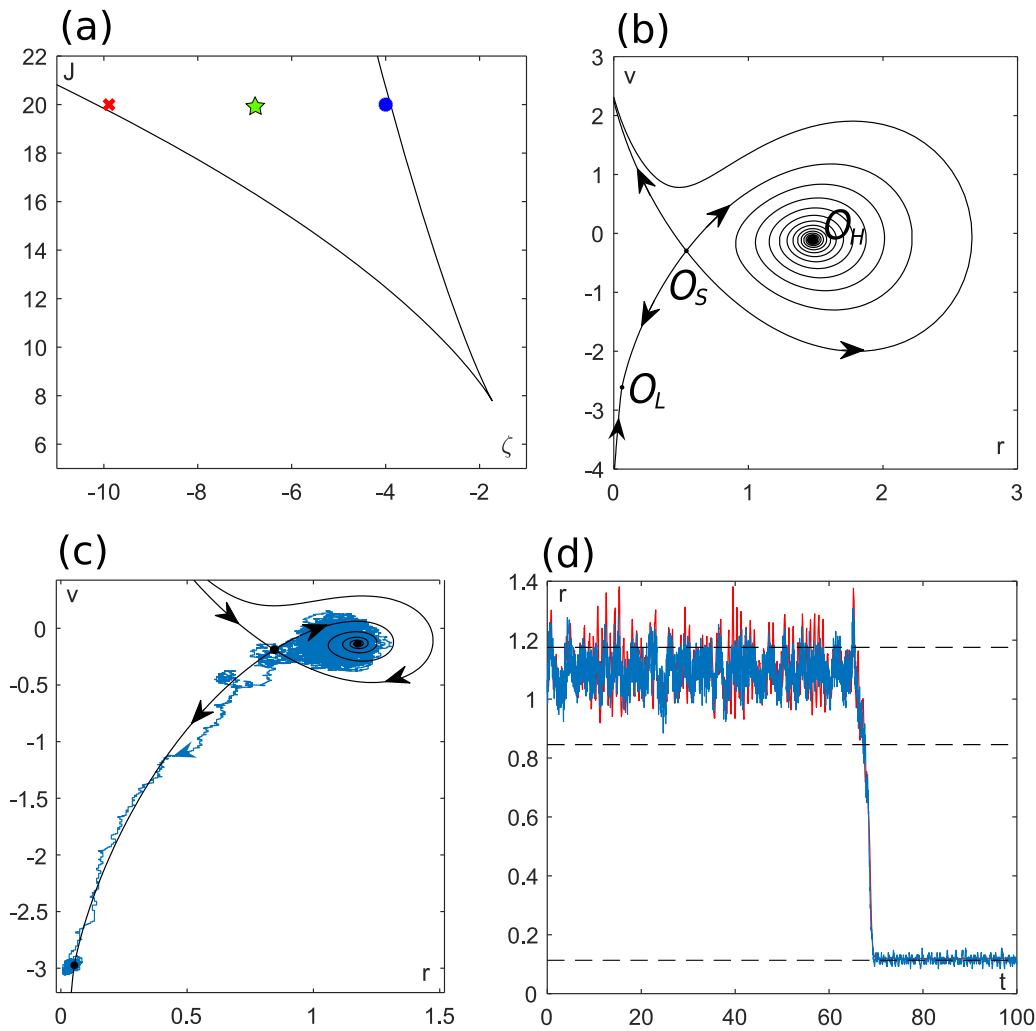
FIG. 1. (a) Bifurcation diagram of the neural mass model (4) for $\Delta = 1$. System is bistable within the region bounded by the curves of saddle-node bifurcations (solid lines). (b) A typical phase portrait of the neural mass system inside the bistability area: two stable steady states O_H and O_L separated by the saddle O_S. (c) Phase portrait of the neural mass model for $J = 20$, $\zeta = -9.89$ [red cross in (a)] and the trajectory of a finite-size network with $N = 400$ (blue line). (d) Filtered activity of the finite-size network with $N = 400$. Blue line: running average with the window width $\Delta t = 0.3$, red line: neural mass model driven by the finite-size network, see Eq. (6). Horizontal dashed lines correspond to steady states of the neural mass model.

Obviously, the likelihood of the dynamical system to switch from one attractor to another under a stochastic perturbation depends on the magnitude of this perturbation and the system's resilience. While the former scales inversely proportional to a square root of the system size, the latter can be roughly estimated as the distance from the system's attractor to the boundary of its attraction basin.[59–61] The latter observation suggests that noise-induced switching is likely to be observed near bifurcations curves where the attractor collides with an unstable state and vanishes.

In system (4), the only possible attractors are steady states, and the bifurcation diagram of this system is depicted in Fig. 1(a).

It contains two saddle-node bifurcation curves, which converge in the codimension-two cusp-point bifurcation point and form a bistability region between the two curves. Inside the bistability area, the system possesses three steady states: a stable node O_L corresponding to low activity (firing rate), another stable steady state O_H, typically a stable focus, corresponding to higher activity, and a saddle O_S separating these two states. A typical phase portrait of the system inside the bistability area is shown in Fig. 1(b). On the lower branch of the saddle-node bifurcation, the high activity state O_H collides with the saddle and vanishes, while the upper saddle-node branch corresponds to the vanishing of the low activity state O_L.

III. NOISE-INDUCED ESCAPE FROM THE HIGH-ACTIVITY STATE

Let us now concentrate on the dynamics of finite-size network. For this case, the set of bias currents η_j is discrete and can be described by the continuous distribution only approximately. Thus, the particular realization of this set might influence the network dynamics. In order to minimize the deviations caused by subsampling and ensure the reproducibility of the results, we generated the set η_j deterministically as it was done in Ref. 33,

$$\eta_j = \zeta + \Delta \tan \frac{\pi(2j - N - 1)}{2(N + 1)}, \qquad (5)$$

where $j = 1, \ldots, N$.

As mentioned before, noise-induced switching should be expected near the bifurcations of the deterministic system. Following this conjecture, we took the parameters inside the bistability region but close to its boundary. First, we take the parameters close to the lower branch of the saddle-node bifurcation, at the point shown by a red cross in Fig. 1(a). The phase portrait of the reduced system for these parameters shown in Fig. 1(c) reveals that the high-activity state O_H is much closer to the saddle separatrix than the low-activity one O_L. Therefore, for a finite-size network, it is natural to expect the noise-induced switching to the low-activity state.

We simulated the finite-size network of $N = 400$ neurons starting from the high-activity steady state of the reduced system. The dynamics of the network is illustrated in Figs. 1(c) and 1(d) and indeed shows noise-induced switching. The system spends some time near the high-activity state demonstrating quite pronounced fluctuations of the activity and then switches to the low-activity state where the fluctuations substantially decrease. The switching in the opposite direction was never observed within a very long simulation time ($t \leq 10^6$).

Two points should be made regarding the results shown in Fig. 1 before a systematic study of noise-induced switching can be performed. First, the microscopic dynamics must be filtered with an appropriate temporal filter in order to observe switching: otherwise, the network activity appears as a series of individual spikes. In Fig. 1(c), we used running average with the time window $\Delta t = 0.3$ selected empirically. Another option would be to use the nested configuration suggested in Ref. 45, in which the finite-size network is considered a part of the infinite one. All the neurons in the infinite network receive input only from the finite network. Obviously, the dynamics of the infinite network are governed by Eqs. (4) with (4b) replaced by

$$\dot{v} = v^2 + \zeta - \pi^2 r^2 + Js(t), \qquad (6)$$

where $s(t)$ is the output of the finite-size network obtained from Eq. (2). Then, the fluctuations of the infinite network represent a filtered version of the shot noise, and the mean-field (neural mass) system represents a natural temporal filter for its observation as illustrated in Fig. 1(d) where it is compared with the output of the running average filter. Note that we further use this neural mass filter in order to avoid tuning of the time window for the running average filter whose optimal width might depend on the system parameters.

The second point which should be taken into account when studying switching due to shot noise is that in the finite-size network, a stable steady state of the neural mass model might not only become metastable but also shift with respect to the one in the neural mass model. This effect is clearly seen in Fig. 1(c) where the "cloud" of the noisy trajectory is obviously centered not in the steady state of the deterministic system but is shifted to the left of it. Similarly, in Fig. 1(d), the high-activity metastable state of the finite size network has an average firing rate lower than that of the high-activity state O_H of the neural mass model. This feature underlines the importance of the proper choice of initial conditions for the study of metastable states in the finite-size network. It might happen that the network initialized to the higher-activity steady state of the neural mass system switches to the low activity very fast, while a metastable state with a much longer lifetime is shifted compared to the neural mass model.

In order to resolve the problem of a potential shift of metastable state, we performed the following procedure. We started from the parameter values deep inside the bistability area where the system is not prone to switching [green asterisk in Fig. 1(a)]. We initialized the system in the high-activity state of the neural mass model and then started to decrease adiabatically the mean bias current ζ from the initial value ζ_0 toward the saddle-node bifurcation until the desired value is reached. Then, we simulated the system for a long time looking for a possible switching to the low-activity state (if it did not happen earlier during the parameter variation).

We considered an ensemble of 1000 networks of a certain size N which allowed to obtain the dependence of the survival probability on time which turned exponential, see Fig. 2(a). The decay rate of the survival probability equals $r = 1/L$, where L is the (average) lifetime. By taking different bias currents ζ, we obtained the dependence of the lifetime of the high-activity state on this parameter. The results presented in Fig. 2(b) for several network sizes N demonstrate transitions from very long lifetimes ($L > 10^4$) when the high-activity state is, in fact, stable to very short lifetimes ($L < 50$) when it effectively vanishes. The transitions are smooth for small networks, while for large networks they become sharper and approach the point of the saddle-node bifurcation of the neural mass model.

Note that for all network sizes, the transition value of ζ is located *inside* the bistability region of the neural mass model. Thus, shot noise effectively reduces the region where the high-activity state exists. It is also instructive to analyze the dependence of the lifetimes vs the network size for the fixed bias current ζ, which is shown in Fig. 2(c). The lifetimes grow exponentially when the network size increases, which is quite natural since the shot noise gets weaker.

IV. NOISE-INDUCED ESCAPE FROM THE LOW-ACTIVITY STATE

An analysis similar to the above one can be applied to the low-activity state in order to study noise-induced switching from this state to the high-activity state. To do so, we first took the parameters inside the bistability region of the neural mass model close to the saddle-node bifurcation of the low-activity state [blue circle in Fig. 1(a)]. Surprisingly, we did not see the switching from the low-activity to high-activity state even for N as small as 100.
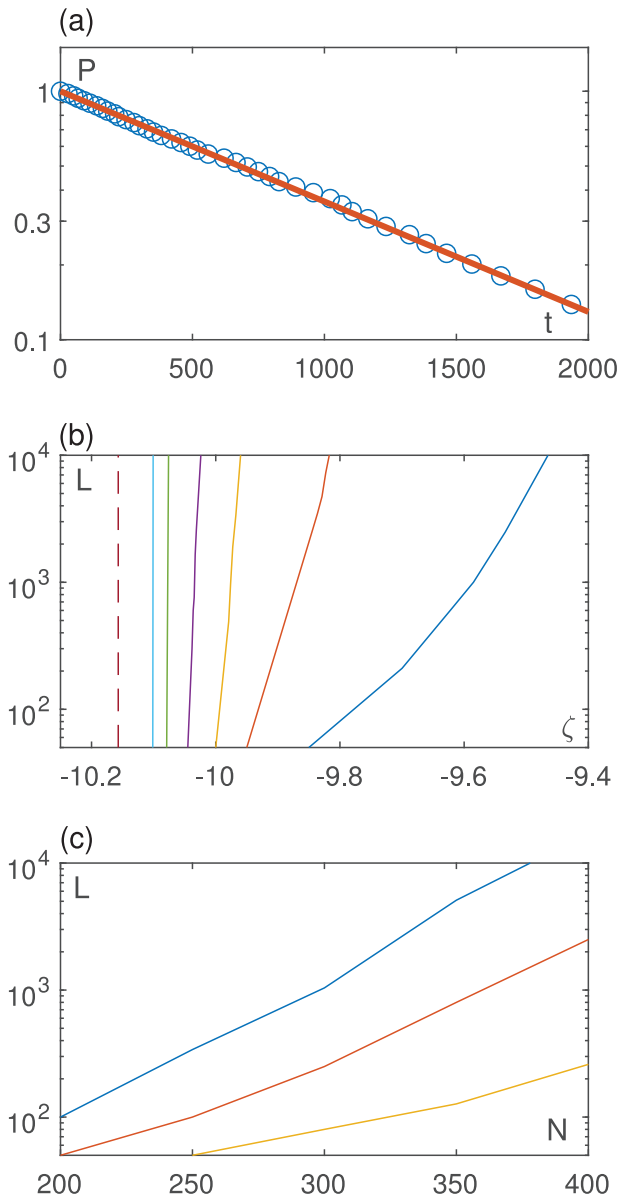
FIG. 2. (a) Blue circles: the survival probability of the high-activity state vs time for $N = 200$ and $\zeta = -9.6$. Note the logarithmic scale of the vertical axis. The red line depicts the approximation $P = e^{-t/L}$ with $L = 978$. (b) The lifetime of the high-activity state vs the mean bias current ζ for different network sizes. Solid lines, right to left: $N = 200, 400, 800, 1600, 3200,$ and 6400. The dashed vertical line shows the bifurcation point of the neural mass model. (c) The lifetime vs the network size for different values of ζ. Solid lines, top to bottom: $\zeta = -9.8$, $\zeta = -9.85$, $\zeta = -9.9$.

Then, we started from the parameter values deep inside the bistability region, initialized the finite-size network near the low-activity state and started to gradually increase the mean bias current. In this setting, we observed the switching in the vicinity to the right branch

of the saddle-node bifurcation curve and measured the lifetimes L of the low-activity state. The results presented in Fig. 3(a) again show a continuous transition from a practically stable state with $L > 10^4$ to a vanishing state with $L < 50$.

However, the shot noise-induced switching from the low-activity state is drastically different from the switching from the high-activity one. Surprisingly, the shot noise sifts the transition *outside* of the bistability region of the neural mass model, which implies *expansion* of the region where the low-activity state exists. The average lifetimes of the low-activity state for different N in Fig. 3(a) indicate that the transition shifts to larger ζ and becomes more smooth as the system size decreases, i.e., as the shot noise grows. To characterize the expansion of the low-activity state, we calculated the parameter value ζ_N for which the network of the size N has a lifetime $L(\zeta_N) = 1000$. The distance from this point to the bifurcation point ζ_∞ of the neural mass model is plotted in Fig. 3(b) vs the network size N in double logarithmic scale. The expansion $\zeta_N - \zeta_\infty$ scales as the inverse square root of the network size, i.e., as the strength of the shot noise. We also plotted the dependence of the lifetime on the network size N for several fixed values of ζ in Fig. 3(c) to show explicitly that increasing the network size destabilizes the metastable state and decreases its lifetime. Comparing these results with Fig. 2(c) one immediately sees that the effect of the shot noise is opposite for the high-activity and the low-activity states.

In order to confirm that extension of the area where the low-activity state exists can be interpreted as the constructive effect of shot noise, we modeled the finite-size network using the stochastic version of the neural mass model suggested in Ref. 45. This model represents Montbrió–Pazó–Roxin system (4) with the second Eq. (4b) replaced by

$$\dot{v} = v^2 + \zeta - \pi^2 r^2 + Jr + J\chi_0(t)/\sqrt{N}, \qquad (7)$$

where $\chi_0(t)$ is the so-called free shot noise. We simulated the stochastic neural mass model near the bifurcation points for different network sizes N. For each network size, the free shot noise was generated as a difference between the output of the (uncoupled) finite-size network and the infinite network receiving the same (constant) input $I_0 = Jr_0$, where r_0 corresponds to the firing rate at the bifurcation point (see the Appendix for the details). The so generated shot noise is a good approximation while the system is close to the low-activity state. Therefore, it can serve for modeling the escape process, although it becomes inadequate as soon as the system reaches the high-activity state. The results for the stochastic neural mass model are presented in Fig. 4(a) and show qualitative similarity with the results for the microscopic system from Fig. 3(b): as the network size N decreases, the transition border shifts to the right and becomes sharper. Interestingly, white noise approximation of the shot noise fails to reproduce this result: if $\chi_0(t)$ is replaced by the white Gaussian noise with the intensity r_0, the transition border shifts in the opposite direction as the network size decreases, see Fig. 4(b). This observation underlines the inadequacy of white noise approximation for massively coupled networks, in contrast to sparse coupling.

We have demonstrated that the role of the shot noise turns out to be substantially different for the high-activity and low-activity regimes of the network. Although in both cases it may
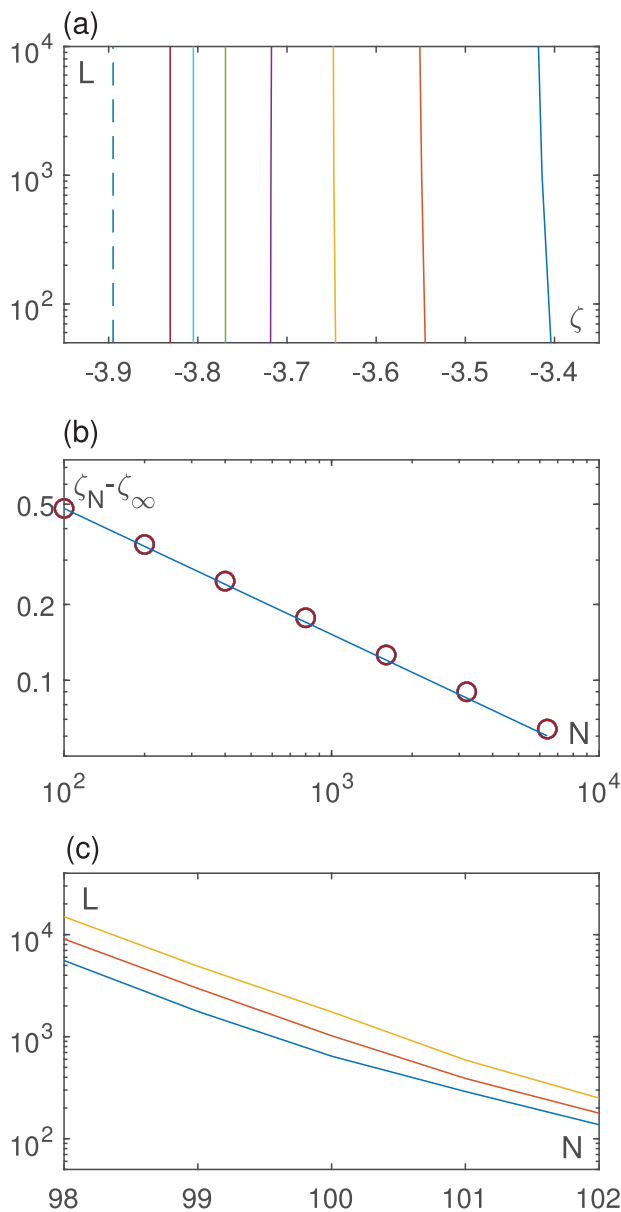
FIG. 4. (a) The lifetime of the low-activity state vs ζ for different N in the stochastic neural mass model (7). Solid lines, right to left: $N = 200, 400, 800,$ and 1600. Vertical dashed line: saddle-node bifurcation of the neural mass model. (b) The same with the shot noise replaced by the white noise. Solid lines, *left to right*: $N = 200, 400, 800,$ and 1600.

FIG. 3. (a) The lifetime of the low-activity state vs ζ for different N. Solid lines, right to left: $N = 100, 200, 400, 800, 1600, 3200,$ and 6400. Vertical dashed line: saddle-node bifurcation of the neural mass model. (b) Red circles: the distance between the point where the lifetime of the lower state equals 10^3 and the bifurcation point of the neural mass model vs the network size. Note the double logarithmic scale. Blue solid lines show the slope $\sim N^{-1/2}$. (c) The lifetime vs the network size for different values of ζ. Solid lines, top to bottom: $\zeta = -3.414$, $\zeta = -3.413, \zeta = -3.412$.

cause noise-induced switching and make the state metastable, it also changes the regions where these states exist, and moreover changes them in an opposite way: while the region of existence of the high-activity state shrinks, the region of existence of the low-activity
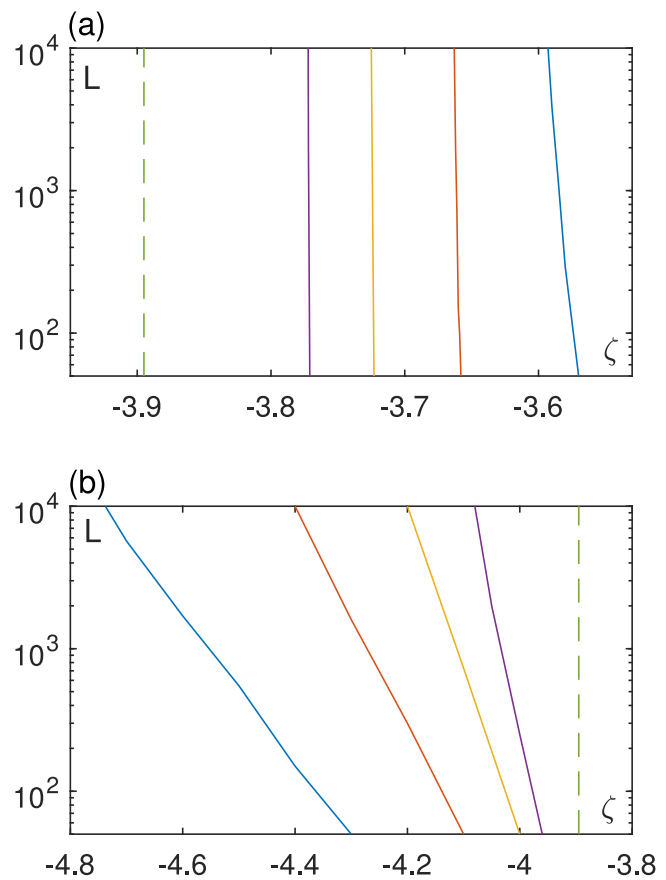
state expands. These two opposite effects are not restricted to certain parameter values but observed generically along the entire branches of the saddle-node bifurcations. Thus, for a finite-size network, the boundary at which the high-activity state vanishes shifts inside the bistability region of the neural mass model, while the boundary at which the low-activity state vanishes moves outside of this region. As a combination of these two effects, the whole bistability region of the finite-size network shifts to higher values of the mean bias current ζ with respect to the thermodynamic case, see Fig. 5(a). Note that we have plotted the lines where the lifetimes of both the states equal $L = 50$. Thus, inside the area limited by these lines the two states coexist, being either metastable or stable.

It is interesting to take a look at the network dynamics near the tip of the bistability area where it is natural to expect recurrent noise-induced switching between the two metastable states. However, the actual scenario is more complicated. When approaching the tip, the two states get close to each other and can no longer be distinguished due to random-like fluctuations, which become larger than
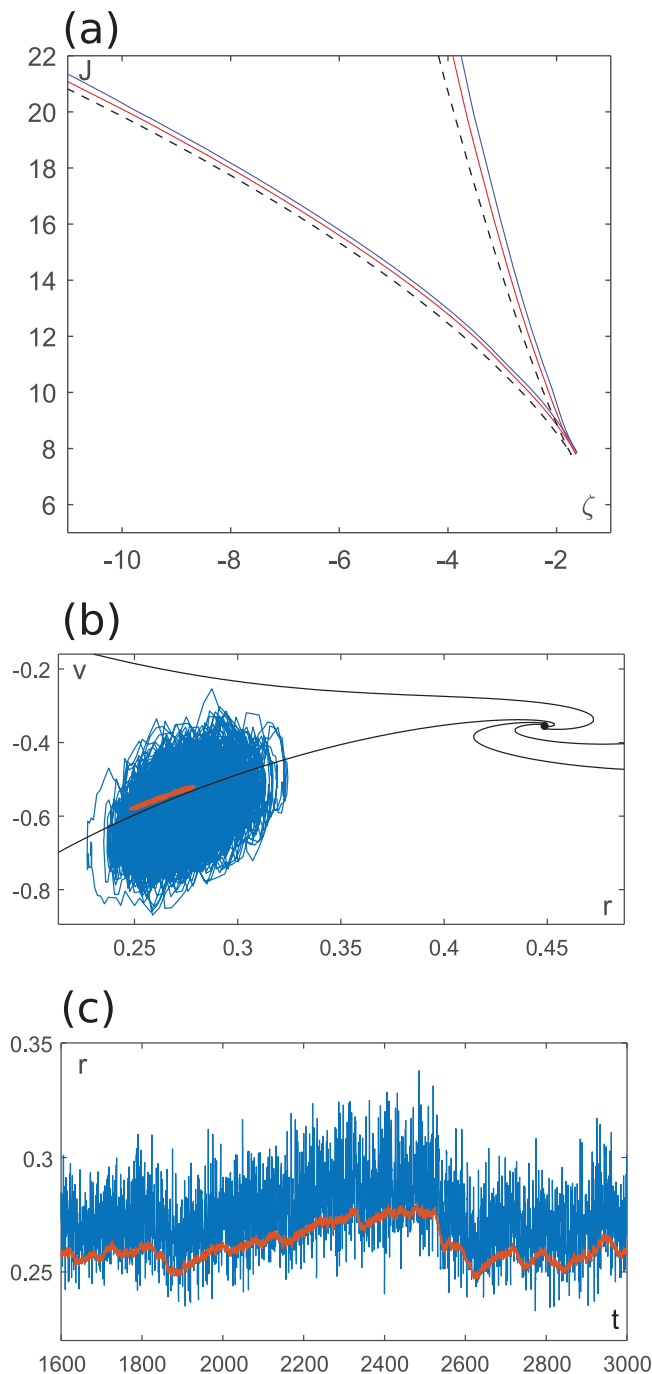
FIG. 5. (a) Borders of existence of the low-activity and high-activity metastable states for the network of $N = 400$ (red lines) and $N = 200$ (blue line) neurons. Dashed lines show the saddle-node bifurcations of the neural mass model. (b) Phase portrait of the neural mass model near the tip of the bistability region and the trajectory of a finite-size network of $N = 400$ neurons ($J = 7.803$, $\zeta = -1.64$). (c) Filtered activity of the same network. Blue line: neural mass model driven by the finite-size network, see Eq. (6). Red line: running average with the window width $\Delta t = 20$.

the distance between the states. Recall that the deterministic system undergoes a cusp bifurcation close to the tip which implies the existence of a neutrally stable central manifold. In the presence of shot noise, the system travels along this manifold while the transversal perturbations fade quickly. An example of such dynamics is illustrated in Figs. 5(b) and 5(c) where the switching-like behavior can be seen only after implementing local time averaging of the network activity over a long temporal window $\Delta t = 20$. Our observations suggest that finite-size fluctuations are probably not enough in order to cause recurrent switching between two well distinguishable states and slow adaptation processes like neural plasticity should be added.[62,63]

V. CONCLUSIONS

Our study shows that the impact of the shot noise due to finite-size effects may be similar to the action of genuine noise on dynamical systems. In particular, it can turn the attractors of an infinite system into metastable states and induce switching between them. The lifetimes of such metastable states depend smoothly on the system parameters.

However, the shot noise may also play a constructive role by extending the parameter area where certain dynamical regimes exist. Here, this effect is observed for the low-activity state of the network which in finite-size networks exits in a larger parameter region than in the thermodynamic limit. It is yet to be understood whether such constructive influence of the shot noise depends on certain features of the macroscopic state or it is related to the effective shift of macroscopic parameters as can be conjectured from Fig. 4(a).

It would also be interesting to compare the shot noise and genuine noise introduced explicitly via stochastic terms on the microscopic or macroscopic level and to find out whether the latter can play a constructive role as well. For example, it would be instructive to compare the constructive effect of shot noise with the effect of noise enhanced stability known for stochastic systems.[64–66] In the context of neural networks, recently it was shown that additive microscopic Gaussian noise can give rise to completely new dynamical regimes in neural networks.[67] It is yet to be established whether the shot noise can play a constructive role in this sense as well. On the other hand, the macroscopic shot noise can provide corrections to neural mass models for networks with microscopic noise.[68–70] The interplay between these two types of noise is another topic worthy of study.

The generality of our results is confined by the assumptions of the model, namely, a network with global, purely excitatory synaptic coupling and mostly sub-threshold dynamics of the single neurons. An important problem following from our study is to attempt to understand the possible constructive role of the shot noise in other network configurations. Our preliminary results indicate similar effects in a network of two populations, an excitatory and an inhibitory ones (will be published elsewhere). However, the situation may be different when a more realistic sparse coupling rather than global coupling is considered. The key difference is that for global connectivity, the neurons receive a common noise, while in sparse networks there are weakly correlated microscopic fluctuations. It is important to understand whether the common noise is indeed

necessary for the effects observed in this study, or similar effects can also be seen for uncorrelated local fluctuations.

AUTHOR DECLARATIONS

Conflict of Interest

The authors have no conflicts to disclose.

Author Contributions

V. V. Klinshov: Conceptualization (equal); Data curation (equal); Formal analysis (equal); Funding acquisition (equal); Investigation (equal); Methodology (equal); Project administration (equal); Resources (equal); Software (equal); Supervision (equal); Validation (equal); Visualization (equal); Writing – original draft (equal); Writing – review & editing (equal). **P. S. Smelov:** Investigation (equal); Software (equal). **S. Yu. Kirillov:** Investigation (equal); Methodology (equal); Visualization (equal).

DATA AVAILABILITY

The data that support the findings of this study are available from the corresponding author upon reasonable request.

APPENDIX: GENERATING A SAMPLE OF THE FREE SHOT NOISE

Here, we describe how to generate a sample of the free shot noise for the finite-size network receiving the constant input I_0. By definition,[45] the free shot noise is the difference between the outputs of the (uncoupled) finite-size network and the infinite network receiving the same input. In the finite-size network receiving the input I_0, the neurons with $\eta_j + I_0 < 0$ are silent, while the neurons with $\eta_j + I_0 > 0$ generate pulses periodically with the frequencies $\nu_j = \sqrt{\eta_j + I_0}/\pi$. Thus, we generate its output as a weighted sum of Dirac combs with these frequencies,

$$s(t) = \frac{1}{N} \sum_j \sum_{k=-\infty}^{\infty} \delta\left(t - k/\nu_j + \theta_j\right),$$

where θ_j is a random phase. For the infinite network receiving the input I_0, the output equals

$$r = \frac{1}{\sqrt{2\pi}} \sqrt{(\zeta + I_0) + \sqrt{(\zeta + I_0)^2 + \Delta^2}},$$

which readily follows from (4). Finally, we generate the free shot noise as

$$\chi_0(t) = \sqrt{N}(s(t) - r).$$

REFERENCES

[1] R. E. Mirollo and S. H. Strogatz, "Synchronization of pulse-coupled biological oscillators," SIAM J. Appl. Math. **50**, 1645–1662 (1990).
[2] D. Hansel and H. Sompolinsky, "Synchronization and computation in a chaotic neural network," Phys. Rev. Lett. **68**, 718 (1992).
[3] R. M. Smeal, G. B. Ermentrout, and J. A. White, "Phase-response curves and synchronized neural networks," Philos. Trans. R. Soc. B **365**, 2407–2422 (2010).
[4] C. C. Canavier, S. Wang, and L. Chandrasekaran, "Effect of phase response curve skew on synchronization with and without conduction delays," Front. Neural Circuits **7**, 194 (2013).
[5] V. Klinshov, L. Lücken, and S. Yanchuk, "Desynchronization by phase slip patterns in networks of pulse-coupled oscillators with delays: Desynchronization by phase slip patterns," Eur. Phys. J.: Spec. Top. **227**, 1117–1128 (2018).
[6] A. V. Andreev, V. A. Maksimenko, A. N. Pisarchik, and A. E. Hramov, "Synchronization of interacted spiking neuronal networks with inhibitory coupling," Chaos, Solitons Fractals **146**, 110812 (2021).
[7] L. F. Abbott and C. van Vreeswijk, "Asynchronous states in networks of pulse-coupled oscillators," Phys. Rev. E **48**, 1483–1490 (1993).
[8] W. Gerstner, "Population dynamics of spiking neurons: Fast transients, asynchronous states, and locking," Neural Comput. **12**, 43–89 (2000).
[9] C. van Vreeswijk, "Partial synchronization in populations of pulse-coupled oscillators," Phys. Rev. E **54**, 5522–5537 (1996).
[10] N. Brunel and X. J. Wang, "What determines the frequency of fast network oscillations with irregular neural discharges? I. Synaptic dynamics and excitation-inhibition balance," J. Neurophysiol. **90**, 415–430 (2003).
[11] V. I. Nekorkin, A. S. Dmitrichev, D. V. Kasatkin, and V. S. Afraimovich, "Relating the sequential dynamics of excitatory neural networks to synaptic cellular automata," Chaos **21**, 43124 (2011).
[12] C. van Vreeswijk and H. Sompolinsky, "Chaos in neuronal networks with balanced excitatory and inhibitory activity," Science (New York, N.Y.) **274**, 1724–6 (1996).
[13] N. Brunel, "Dynamics of sparsely connected networks of excitatory and inhibitory spiking neurons," J. Comput. Neurosci. **8**, 183–208 (2000).
[14] D. S. Shchapin and V. I. Nekorkin, "Parametrically excited chaotic spike sequences and information aspects in an ensemble of Fitzhugh–Nagumo neurons," JETP Lett. **113**, 418–422 (2021).
[15] E. Ullner and A. Politi, "Self-sustained irregular activity in an ensemble of neural oscillators," Phys. Rev. X **6**, 011015 (2016).
[16] A. Politi, E. Ullner, and A. Torcini, "Collective irregular dynamics in balanced networks of leaky integrate-and-fire neurons," Eur. Phys. J.: Spec. Top. **227**, 1185–1204 (2018).
[17] A. Compte, N. Brunel, P. S. Goldman-Rakic, and X. J. Wang, "Synaptic mechanisms and network dynamics underlying spatial working memory in a cortical network model," Cereb. Cortex **10**, 910–923 (2000).
[18] V. V. Klinshov and V. I. Nekorkin, "Working memory in the network of neuron-like units with noise," Int. J. Bifurcation Chaos **18**, 2743–2752 (2008).
[19] H. R. Wilson and J. D. Cowan, "Excitatory and inhibitory interactions in localized populations of model neurons," Biophys. J. **12**, 1–24 (1972).
[20] S. ichi Amari, "Dynamics of pattern formation in lateral-inhibition type neural fields," Biol. Cybern. **27**, 77–87 (1977).
[21] B. H. Jansen and V. G. Rit, "Electroencephalogram and visual evoked potential generation in a mathematical model of coupled cortical columns," Biol. Cybern. **73**, 357–366 (1995).
[22] J. Eggert and J. L. V. Hemmen, "Modeling neuronal assemblies: Theory and implementation," Neural Comput. **13**, 1923–1974 (2001).
[23] W. Gerstner and W. M. Kistler, *Spiking Neuron Models: Single Neurons, Populations, Plasticity* (Cambridge University Press, 2002).
[24] A. V. Chizhov and L. J. Graham, "Population model of hippocampal pyramidal neurons, linking a refractory density approach to conductance-based neurons," Phys. Rev. E **75**, 011924 (2007).

[25]S. E. Boustani and A. Destexhe, "A master equation formalism for macroscopic modeling of asynchronous irregular activity states," Neural Comput. **21**, 46–100 (2009).

[26]M. di Volo, A. Romagnoni, C. Capone, and A. Destexhe, "Biologically realistic mean-field models of conductance-based networks of spiking neurons with adaptation," Neural Comput. **31**, 653–680 (2019).

[27]H. Hasegawa, "Generalized rate-code model for neuron ensembles with finite populations," Phys. Rev. E **75**, 051904 (2007).

[28]J. nosuke Teramae, Y. Tsubo, and T. Fukai, "Optimal spike-based communication in excitable networks with strong-sparse and weak-dense links," Sci. Rep. **2**, 485 (2012).

[29]V. Klinshov and I. Franović, "Mean-field dynamics of a random neural network with noise," Phys. Rev. E **92**, 062813 (2015).

[30]I. Franović, O. V. Maslennikov, I. Bačić, and V. I. Nekorkin, "Mean-field dynamics of a population of stochastic map neurons," Phys. Rev. E **96**, 012226 (2017).

[31]E. Ott and T. M. Antonsen, "Low dimensional behavior of large systems of globally coupled oscillators," Chaos **18**, 37113 (2008).

[32]E. Ott and T. M. Antonsen, "Long time evolution of phase oscillator systems," Chaos **19**, 23117 (2009).

[33]E. Montbrió, D. Pazó, and A. Roxin, "Macroscopic description for networks of spiking neurons," Phys. Rev. X **5**, 021028 (2015).

[34]T. B. Luke, E. Barreto, and P. So, "Complete classification of the macroscopic behavior of a heterogeneous network of theta neurons," Neural Comput. **25**, 3207–3234 (2013).

[35]C. R. Laing, "Derivation of a neural field model from a network of theta neurons," Phys. Rev. E **90**, 010901 (2014).

[36]F. Devalle, A. Roxin, and E. Montbrió, "Firing rate equations require a spike synchrony mechanism to correctly describe fast oscillations in inhibitory networks," PLoS Comput. Biol. **13**, e1005881 (2017).

[37]H. Bi, M. Segneri, M. di Volo, and A. Torcini, "Coexistence of fast and slow gamma oscillations in one population of inhibitory spiking neurons," Phys. Rev. Res. **2**, 13042 (2020).

[38]M. Segneri, H. Bi, S. Olmi, and A. Torcini, "Theta-nested gamma oscillations in next generation neural mass models," Front. Comput. Neurosci. **14**, 47 (2020).

[39]S. Keeley, Á. Byrne, A. Fenton, and J. Rinzel, "Firing rate models for gamma oscillations," J. Neurophysiol. **121**, 2181–2190 (2019).

[40]Á. Byrne, M. J. Brookes, and S. Coombes, "A mean field model for movement induced changes in the beta rhythm," J. Comput. Neurosci. **43**, 143–158 (2017).

[41]H. Schmidt, D. Avitabile, E. Montbrió, and A. Roxin, "Network mechanisms underlying the role of oscillations in cognitive tasks," PLoS Comput. Biol. **14**, e1006430 (2018).

[42]H. Taher, A. Torcini, and S. Olmi, "Exact neural mass model for synaptic-based working memory," PLoS Comput. Biol. **16**, e1008533 (2020).

[43]M. Gerster, H. Taher, A. Škoch, J. Hlinka, M. Guye, F. Bartolomei, V. Jirsa, A. Zakharova, and S. Olmi, "Patient-specific network connectivity combined with a next generation neural mass model to test clinical hypothesis of seizure propagation," Front. Syst. Neurosci. **15**, 675272 (2021).

[44]Á. Byrne, R. D. O'Dea, M. Forrester, J. Ross, and S. Coombes, "Next-generation neural mass and field modeling," J. Neurophysiol. **123**, 726–742 (2020).

[45]V. V. Klinshov and S. Y. Kirillov, "Shot noise in next-generation neural mass models for finite-size networks," Phys. Rev. E **106**, L062302 (2022).

[46]B. Lindner, J. García-Ojalvo, A. Neiman, and L. Schimansky-Geier, "Effects of noise in excitable systems," Phys. Rep. **392**, 321–424 (2004).

[47]H. A. Kramers, "Brownian motion in a field of force and the diffusion model of chemical reactions," Physica **7**, 284–304 (1940).

[48]L. S. Tsimring and A. Pikovsky, "Noise-induced dynamics in bistable systems with delay," Phys. Rev. Lett. **87**, 250602 (2001).

[49]T. Schwalger and B. Lindner, "Higher-order statistics of a bistable system driven by dichotomous colored noise," Phys. Rev. E **78**, 21121 (2008).

[50]O. D'Huys, T. Jüngling, and W. Kinzel, "Stochastic switching in delay-coupled oscillators," Phys. Rev. E **90**, 032918 (2014).

[51]I. Franović and V. Klinshov, "Slow rate fluctuations in a network of noisy neurons with coupling delay," EPL **116**, 48002 (2016).

[52]I. Franović and V. Klinshov, "Clustering promotes switching dynamics in networks of noisy neurons," Chaos **28**, 023111 (2018).

[53]V. Klinshov, D. Shchapin, and O. D'Huys, "Mode hopping in oscillating systems with stochastic delays," Phys. Rev. Lett. **125**, 034101 (2020).

[54]I. Franović, S. Yanchuk, S. Eydam, I. Bačić, and M. Wolfrum, "Dynamics of a stochastic excitable system with slowly adapting feedback," Chaos **30**, 083109 (2020).

[55]E. M. Izhikevich, *Dynamical Systems in Neuroscience* (MIT Press, 2008), p. 441.

[56]D. Hansel and G. Mato, "Asynchronous states and the emergence of synchrony in large networks of interacting excitatory and inhibitory neurons," Neural Comput. **15**, 1–56 (2003).

[57]I. Ratas and K. Pyragas, "Macroscopic self-oscillations and aging transition in a network of synaptically coupled quadratic integrate-and-fire neurons," Phys. Rev. E **94**, 032215 (2016).

[58]B. Pietras, "Pulse shape and voltage-dependent synchronization in spiking neuron networks," arXiv:2304.09813 (2023).

[59]V. V. Klinshov, V. I. Nekorkin, and J. Kurths, "Stability threshold approach for complex dynamical systems," New J. Phys. **18**, 13004 (2016).

[60]V. V. Klinshov, S. Kirillov, J. Kurths, and V. I. Nekorkin, "Interval stability for complex systems," New J. Phys. **20**, 043040 (2018).

[61]N. L. Lundström, "How to find simple nonlocal stability and resilience measures," Nonlinear Dyn. **93**, 887–908 (2018).

[62]V. Schmutz, W. Gerstner, and T. Schwalger, "Mesoscopic population equations for spiking neural networks with synaptic short-term plasticity," J. Math. Neurosci. **10**, 1–32 (2020).

[63]B. Pietras, V. Schmutz, and T. Schwalger, "Mesoscopic description of hippocampal replay and metastability in spiking neural networks with short-term plasticity," PLoS Comput. Biol. **18**, e1010809 (2022).

[64]R. N. Mantegna and B. Spagnolo, "Noise enhanced stability in an unstable system," Phys. Rev. Lett. **76**, 563–566 (1996).

[65]A. Fiasconaro, B. Spagnolo, and S. Boccaletti, "Signatures of noise-enhanced stability in metastable states," Phys. Rev. E **72**, 61110 (2005).

[66]I. Bačić and I. Franović, "Two paradigmatic scenarios for inverse stochastic resonance," Chaos **30**, 033123 (2020).

[67]D. S. Goldobin, M. di Volo, and A. Torcini, "Reduction methodology for fluctuation driven population dynamics," Phys. Rev. Lett. **127**, 038301 (2021).

[68]D. S. Goldobin, I. V. Tyulkina, L. S. Klimenko, and A. Pikovsky, "Collective mode reductions for populations of coupled noisy oscillators," Chaos **28**, 101101 (2018).

[69]P. Clusella and E. Montbrió, "Regular and sparse neuronal synchronization are described by identical mean field dynamics," arXiv:2208.05515 (2022).

[70]B. Pietras, A. Pikovsky *et al.*, "Exact finite-dimensional description for networks of globally coupled spiking neurons," Phys. Rev. E **107**, 24315 (2023).